Modeling of G Protein-Coupled Receptors Using Crystal Structures: From Monomers to Signaling Complexes

2

Angel Gonzalez, Arnau Cordomí, Minos Matsoukas, Julian Zachmann, and Leonardo Pardo

Abstract

G protein–coupled receptors constitute a large and functionally diverse family of transmembrane proteins. They are fundamental in the transfer of extracellular stimuli to intracellular signaling pathways and are among the most targeted proteins in drug discovery. Recent advances in crystallization methods have permitted to resolve the molecular structure of several members of the family. This chapter focuses on the impact of these structures in the use of homology modeling techniques for building three-dimensional models of homologous G protein–coupled receptors, higher order oligomers, and their complexes with ligands and signaling proteins.

Keywords

Transmembrane helices • Homology modeling • Conformation • Ligand binding • Activation mechanism

2.1 Introduction

Membrane receptors coupled to guanine nucleotide-binding proteins (commonly known as G protein-coupled receptors, GPCRs) comprise one of the widest and most adaptable families of cellular sensors, as they are able to mediate a wide range of transmembrane signal transduction processes (Kristiansen 2004). GPCRs are present in almost every eukaryotic organism, including fungi and plants. They are highly diversified in mammalian genomes with current estimates of about 1,000 genes (2–3 % of the human proteome) (Fredriksson and Schioth 2005). GPCRs transduce sensory signals of external origin such as odors, pheromones, or tastes; and endogenous signals such as neurotransmitters, (neuro)peptides, proteases, glycoprotein hormones, purine ligands and ions, among others. The response is operated through second messenger cascades controlled by different heterotrimeric guanine nucleotide-binding proteins (G-proteins) coupled at their intracellular regions (Oldham and Hamm 2008). Due to their relevance to cellular physiology (Smit et al. 2007) and their accessibility from the extracellular environment, membrane proteins

A. Gonzalez • A. Cordomí • M. Matsoukas • J. Zachmann • L. Pardo (✉)
Laboratori de Medicina Computacional, Unitat de Bioestadística, Facultat de Medicina, Universitat Autònoma de Barcelona, 08193 Bellaterra, Spain
e-mail: Leonardo.Pardo@uab.es

M. Filizola (ed.), *G Protein-Coupled Receptors - Modeling and Simulation*, Advances in Experimental Medicine and Biology 796, DOI 10.1007/978-94-007-7423-0_2,

represent a significant portion of therapeutic drug targets (Arinaminpathy et al. 2009; Imming et al. 2006).

2.2 The Structure of G Protein-Coupled Receptors

Significant advances in crystallization of GPCRs (Day et al. 2007; Serrano-Vega et al. 2008) have permitted to elucidate the crystal structures of many receptors (Table 2.1) (see (Katritch et al. 2012, 2013) for recent reviews). All these structures share the common architecture of seven plasma membrane-spanning (or transmembrane) domains (TMs, which also terms this family of proteins as 7TM receptors) connected to each other with three extracellular (ECL) and three intracellular loops (ICL), a disulphide bridge between ECL 2 and TM 3, and a cytoplasmic C–terminus containing an α-helix (Hx8) parallel to the cell membrane. In addition, GPCRs contain an extracellular N-terminal region (N-terminus) and an intracellular C-terminal tail (C-tail).

2.3 Homology Modeling of G Protein-Coupled Receptors

Because of the limited high-resolution structural information on GPCRs, computational techniques to predict their structure from the amino acid sequence are a valuable tool (Pieper et al. 2013). Recently, de novo techniques using evolutionary constraints have been applied to predict 3D structures of TM proteins (Hopf et al. 2012). However, homology models of proteins with unknown experimental structure can also be built from homologous proteins of known structure and similar sequence (templates). This method is based on the fact that in homologous proteins, structure is more conserved than sequence. Thus, in general, homologous proteins with a sequence identity above 35 % have a similar 3D structure (Krissinel and Henrick 2004). Because membrane proteins contain only two types of folds in their TM domains, α-helix bundles and β-barrels, a significant set of membrane proteins maintains a strong conservation of the TM structure even at low sequence identity (<20 %) (Olivella et al. 2013).

The GPCR family is not an exception. All crystal structures preserve analogous secondary/tertiary structures at the seven-helical-bundle domain (Fig. 2.1) despite the percentage of sequence identity in the TM segments is very low (Mobarec et al. 2009; Gonzalez et al. 2012). Structure conservation in the GPCR family is associated, in contrast to other proteins, to the presence of at least one highly conserved amino acid in each helix (Mirzadegan et al. 2003): N in TM1 (present in 98 % of the sequences), D in TM2 (93 %), R in TM3 (95 %), W in TM4 (96 %), P in TM5 (76 %), P in TM6 (98 %), and P in TM7 (93 %). This feature was used by Ballesteros and Weinstein (1995) to define a general numbering scheme consisting of two numbers: the first (1 through 7) corresponds to the helix in which the amino acid of interest is located; the second indicates its position relative to the most conserved residue in the helix, arbitrarily assigned to 50. Significantly, the position of these highly conserved amino acids in each helix is the same in the superimposition of the currently available crystal structures (Fig. 2.1). This finding validates the use of these amino acids as reference points in TM sequence alignments (instead of the common procedure of using substitution matrices and fast sequence similarity search algorithms) (see red box in Fig. 2.2), and in the construction of homology models of GPCRs with unknown structure (de la Fuente et al. 2010; Blattermann et al. 2012).

2.4 The Conformation of Transmembrane Helices in G Protein-Coupled Receptors

Figure 2.1 shows the superimposition of the TM domain of representative crystal structures. Clearly, the structure of the cytoplasmic part is highly conserved. This structural conservation correlates with the fact that most conserved residues are clustered in the central and

Table 2.1 Crystal structures of G protein coupled receptors

Receptor	Ligand	PDB	Reference
Rhodopsin			
Bovine Rhodopsin (bRho)	11-*cis* retinal	1F88, 1GZM	Palczewski et al. (2000) and Li et al. (2004)
Squid Rhodopsin (sRho)	11-*cis* retinal	2Z73	Murakami and Kouyama (2008)
Opsin		3CAP	Park et al. (2008)
Opsin + transducin peptide		3DQB	Scheerer et al. (2008)
Constitutively active rhodopsin		2X72	Standfuss et al. (2011)
Metarhodopsin II	11-*trans* retinal	3PXO	Choe et al. (2011)
Metarhodopsin II + transducin peptide	11-*trans* retinal	3PQR	Choe et al. (2011)
Biogenic amine receptors			
β_1-adrenergic (β_1AR)	Cyanopindolol	2VT4	Warne et al. (2008)
β_1AR	Isoprenaline	2Y03	Warne et al. (2011)
β_1AR homo-oligomer		4GPO	Huang et al. (2013)
β_2-adrenergic (β_2AR)	Carazolol	2RH1	Cherezov et al. (2007) and Rosenbaum et al. (2007)
β_2AR + nanobody	BI-167107	3POG	Rasmussen et al. (2011a)
β_2AR + Gs	BI-167107	3SN6	Rasmussen et al. (2011b)
Dopamine D3 (D3R)	Eticlopride	3PBL	Chien et al. (2010)
Histamine H_1 (H_1R)	Doxepin	3RZE	Shimamura et al. (2011)
Muscarinic M_2 (M_2R)	3-quinuclidinyl-benzilate	3UON	Haga et al. (2012)
Muscarinic M_3 (M_3R)	Tiotropium	4DAJ	Kruse et al. (2012)
Serotonin $5HT_{1B}$ ($5HT_{1B}$R)	Ergotamine	4IAR	Wang et al. (2013a)
Serotonin $5HT_{1B}$ ($5HT_{2B}$R)	Ergotamine	4IB4	Wacker et al. (2013)
Nucleotide			
Adenosine A_{2A} (A_{2A}R)	ZM241385	3EML	Jaakola et al. (2008)
A_{2A}R	UK-432097	3QAK	Xu et al. (2011)
A_{2A}R + Na^+	ZM241385	4EIY	Liu et al. (2012)
Peptide receptors			
CXCR4	CVX15	3OE0	Wu et al. (2010)
CXCR4	IT1t	3ODU	Wu et al. (2010)
μ-opioid (μ-OR)	β-funaltrexamine	4DKL	Manglik et al. (2012)
κ-opioid (κ-OR)	JDTic	4DJH	Wu et al. (2012)
δ-opioid (δ-OR)	Naltrindole	4EJ4	Granier et al. (2012)
Nociceptin/orphanin FQ	C-24	4EA3	Thompson et al. (2012)
Neurotensin1 (NTSR1)	Neurotensin (8–13)	4GRV	White et al. (2012)
Protease-activated receptor 1 (PAR1)	Vorapaxar	3VW7	Zhang et al. (2012)
Lipid			
Sphingosine S1P ($S1P_1$R)	ML056	3V2Y	Hanson et al. (2012)
Frizzled (class F)			
Smoothened (SMO)	LY2940680	4JKV	Wang et al. (2013b)

intracellular regions of the receptor (Mirzadegan et al. 2003). In contrast, there is a low degree of sequence conservation among different GPCRs at their extracellular domains. Accordingly, the structure of the extracellular part of TM helices is more divergent. We have previously suggested that GPCRs, during their evolution, have evolved to adjust the structural characteristics of their cognate ligands, by customizing a preserved scaffold (7TM receptors) through *conformational plasticity* (Deupi et al. 2007). We use this term to describe the structural differences

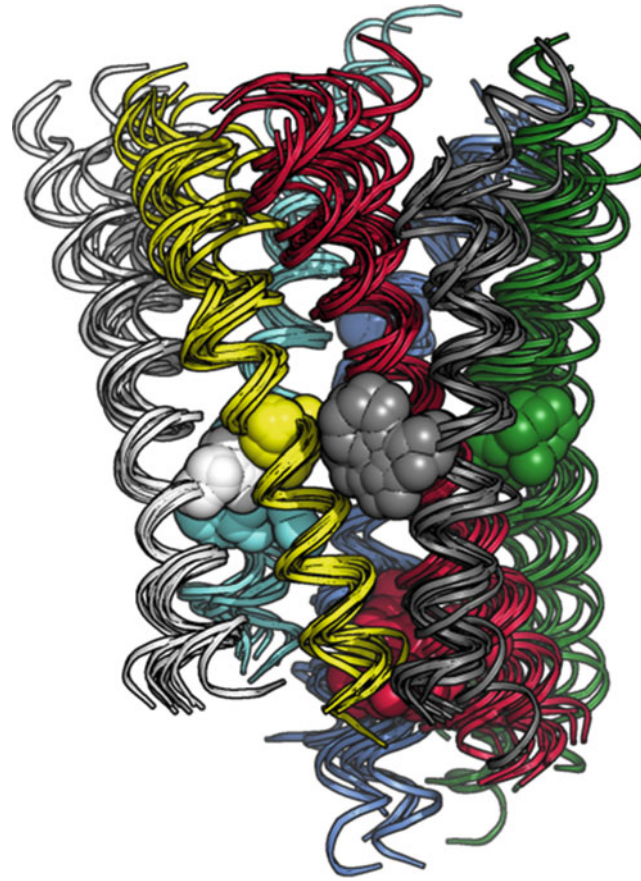

Fig. 2.1 Comparison of the TM bundle of GPCRs. The structures of bRho (PDB code 1U19), β_2R (2RH1), D_3R (3PBL), H_1R (3RZE), M_2R, $5HT_{1b}$R (4IAR), A_{2A}R (4EIY), CXCR4 (3ODU), μOR (4DKL), NTSR1 (4GRV), PAR1 (3VW7), and $S1P_1$R (3V2Y) are shown. The colour code of the helices is TMs 1 in *white*, 2 in *yellow*, 3 in *red*, 4 in *grey*, 5 in *green*, 6 in *dark blue*, and 7 in *light blue*. The highly conserved N1.50 (in *white*), D2.50 (in *yellow*), R3.50 (in *red*), W4.50 (in *grey*), P5.50 (in *green*), P6.50 (in *dark blue*), and P7.50 (in *light blue*) are shown as spheres

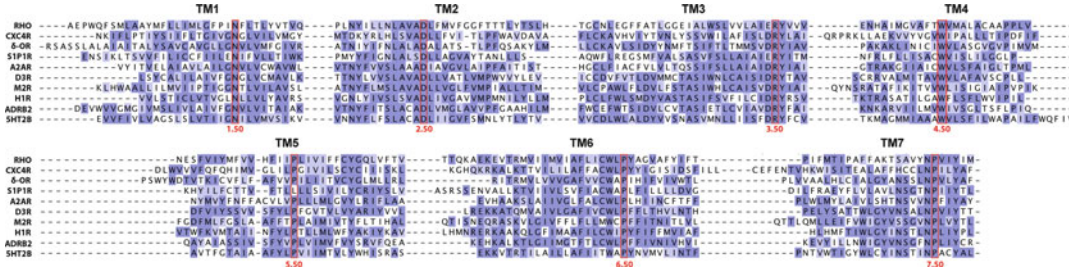

Fig. 2.2 Sequence alignments of TMs 1–7 of GPCRs with known structures. The highly conserved amino acids in each helix, used as reference points in TM sequence alignments are boxed in *red*

among different receptor subfamilies within the extracellular side, near the binding site crevices, responsible for recognition and selectivity of diverse ligands.

Moreover, comparison among the crystal structures of GPCRs revealed backbone anomalies, in the form of kinks and bulges, in the majority of TM helices. These non-canonical elements are frequent in TM proteins, modulating the polytopic membrane protein architecture (Riek et al. 2001). Deviations from the regular α-helical context have been associated to prolines (Von Heijne 1991), glycines (Senes et al. 2000), serines and threonines (Deupi et al. 2004, 2010), or to the insertion or deletions (indels) of residues within the TMs (Deville et al. 2009). Moreover, specific intra- and interhelical interactions involving polar side

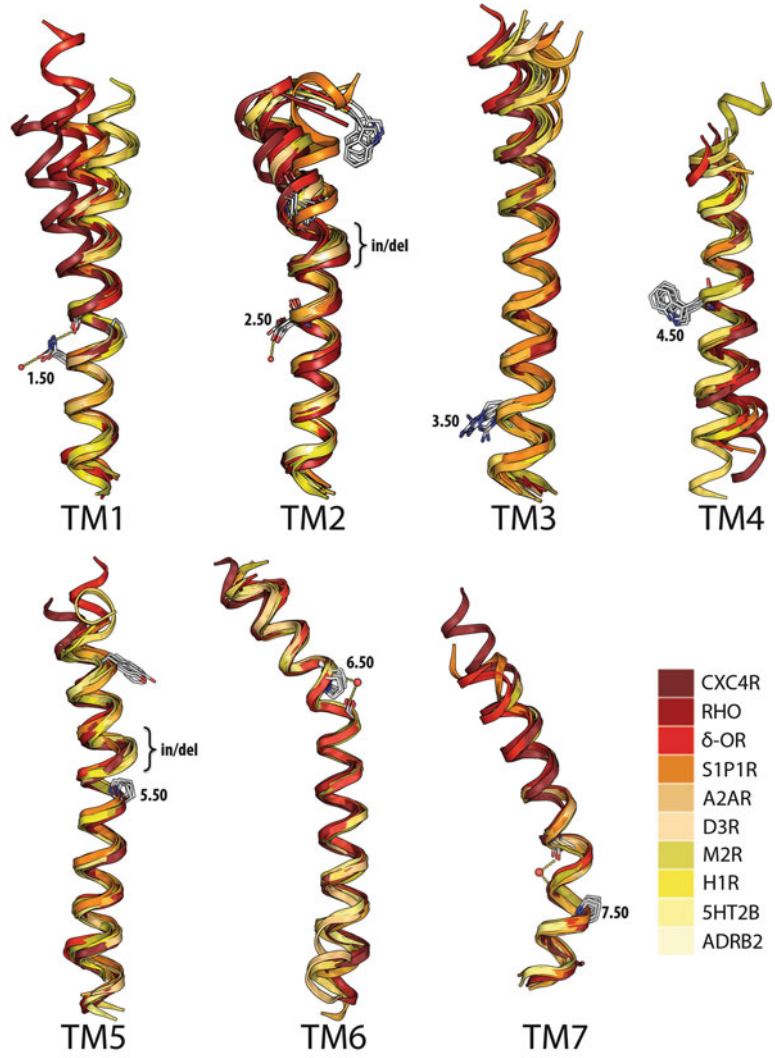

Fig. 2.3 Comparison of individual TM helices in representative structures of the inactive state of GPCRs. The most conserved domain of the helices is superimposed. The crystal structures of GPCRs revealed backbone anomalies, in the form of kinks and bulges, in the majority of TM helices

chains, backbone carbonyls, disulphide bridges and, in some cases, structural water molecules embedded in the TM bundle (Pardo et al. 2007) also cause these distortions. Here we present a detailed analysis of these distortions and their implication in modeling other GPCRs. Figure 2.3 shows the superimposition of the more conserved part of individual TM helices in representative structures of the inactive state of GPCRs.

2.4.1 Transmembrane Helix 1

The extracellular region of TM1 displays a bending propensity in some of the crystal structures (Fig. 2.3). It appears shifted towards the central axis of the receptor in Rho, $A_{2A}R$, CXCR4, opioid receptors, NTSR1, and PAR1. The major displacement of TM1 corresponds to CXCR4 due to the formation of a disulphide bond between the C28 in the N-terminal region and $C274^{7.25}$ in TM7 (Wu et al. 2010). In contrast, TM1 is pointing outside of the bundle in biogenic amine receptors. The highly conserved $N^{1.50}$ (97 % in class A non-olfactory GPCRs) most probably influences the packing of the TM bundle (see Fig. 2.3) since its $N_{\delta 2}$-H atoms act as hydrogen bond donors in the interaction with the backbone carbonyl oxygen of residues at positions 1.46 and 7.46, linking TMs 1 and 7. Moreover, $O_{\delta 1}$ of

$N^{1.50}$ interacts with the highly conserved $D^{2.50}$ (in 92 % of the sequences), via a conserved water molecule, linking TMs 1 and 2. Previous studies have shown that interactions involving a polar Asn side chain provide a strong thermodynamic driving force for membrane helix association (Choma et al. 2000).

2.4.2 Transmembrane Helix 2 – Extracellular Loop 1

The shape of TM2 at the extracellular part, which bends towards TM1 and leans away from TM3, is similar in all structures (Fig. 2.3); despite the amino acid sequence is strongly divergent with, for instance, Pro residues at either position 2.58 (CXCR4, opioid receptors, PAR1), 2.59 (biogenic amine receptors, NTSR1) or 2.60 (sRho). The only exception is TM2 of $A_{2A}R$, which contains Pro at position 2.59 but kinks towards TM3 due to the Cys-bridge between ECL1 and ECL2 exclusive of this family (not shown); and TM2 of $S1P_1R$ that lacks Pro in the helix (see below). Contrarily to $S1P_1R$, the also Pro-lacking bRho and muscarinic receptors possess TM2 structurally similar to the other Pro-containing receptors due to the presence of the GGxTT motif in bRho and $N^{2.59}$ in muscarinic receptors that hydrogen bonds the backbone carbonyl at position 2.55 (Gonzalez et al. 2012). Interestingly, the superimposition of structures reveals that the highly $D^{2.50}$ and the Pro residue located at position 2.58, 2.59 or 2.60 are perfectly overlaid (Gonzalez et al. 2012). Thus, the backbone helical conformation of the amino acids located between these two residues must differ. In this region, TM2 of CXCR4, opioid receptors, and PAR1 adopts a 3_{10} or tight turn (~3.0 residues per turn), TM2 of biogenic amine receptors and NTSR1 adopts a π-bulge or wide turn (~4.8 residues per turn), and TM2 of sRho presents an extreme distortion (~9 residues per turn) characterized by a *cis* $P^{2.60}$ backbone conformation, which is stabilized by two water molecules (Gonzalez et al. 2012). In contrast to these receptors, $S1P_1R$ contains a canonical α-helix at the extracellular part (~3.6 residues per turn). This conformation of TM2 moves its extracellular part away from the TM bundle, relative to the other structures, and modifies the orientation of the side chains at the extracellular side. In order to translate these structural observations into the sequence space, a two-residue gap in the sequences of $S1P_1R$, CXCR4, opioid receptors and PAR1, or one-residue gap in the sequences of bRho, biogenic amine receptors and NTSR1, relative to sRho, must be inserted (Gonzalez et al. 2012) (Fig. 2.2).

Importantly, the conserved Trp residue in ECL1, part of the (W/F) × (F/L)G motif previously identified (Klco et al. 2006), points toward the helical bundle, between TMs 2 and 3, in the crystal structures with the exception of $S1P_1R$ (not shown).

2.4.3 Transmembrane Helix 3

TM3 is the longest and most tilted helix in the receptor structures. No major deviations among structures are observed with the exception of $A_{2A}R$, due to the Cys-bridge between ECL1 and ECL2 exclusive of this family (see above). The highly conserved $C^{3.25}$ forms a disulphide bridge with a Cys residue located at various positions in ECL2. The cytoplasmic side of TM3 contains the highly conserved (D/E)$R^{3.50}$(Y/W) motif involved in receptor activation (see below). Importantly, the central location of TM3 within the TM bundle allows the helix to interact with the ligand at the extracellular part and with the G protein at the intracellular part (Venkatakrishnan et al. 2013).

2.4.4 Transmembrane Helix 4

TM4, the shortest helix, is almost perpendicular to the membrane. However, significant structural divergences at the extracellular part of TM 4 are found among structures, which may be related to the structural requirements necessary to accommodate the diverse ECL2 architectures

(see below). For instance, in contrast to TM4 of other biogenic amine receptors, TM4 of muscarinic receptors bends towards outside of the bundle, away from TM3, due to the hydrogen bond interactions between the side chain of $Q^{4.65}$ and the backbone carbonyl oxygen at position 4.62. Significantly, the shape of TM4 at the extracellular part, in peptide receptors (in which ECL2 is formed by two β-strands, see below), bends towards TM3. In CXCR4, TM4 is longer and substantially deviate from the conformation observed in other peptide receptors.

2.4.5 Transmembrane Helix 5

$P^{5.50}$ (conserved in 76 % of the rhodopsin-like sequences) induces a local opening of TM5, at the 5.43–5.48 turn (Pro-unwinding), in all crystal structures except $S1P_1R$ (see below), which has been proposed to be involved in the mechanism of ligand-induced receptor activation (Sansuk et al. 2011; Rasmussen et al. 2011a). Thus, $P^{5.50}$ triggers a π-bulge or wide turn conformation (∼5 residues per turn). However, $A_{2A}R$ displays an extended opening of TM5 from positions 5.35–5.48, in contrast to other $P^{5.50}$-containing structures in which the opening of the helix is restricted to the 5.43–5.48 range of amino acids.

Moreover, $P^{5.50}$ is absent in melanocortin, glycoprotein hormone, lysosphingolipid, prostanoid, and cannabinoid receptors. In these cases, the similarly conserved $Y^{5.58}$ (73 % of the sequences), functionally involved in the stabilization of the active state of the receptor by interacting with $R^{3.50}$ of the (D/E)RY motif in TM3, as revealed by the crystal structures of β_2AR in complex with Gs (Rasmussen et al. 2011b) and the ligand-free opsin (Park et al. 2008), is used as reference for sequence alignment of TM5 (Fig. 2.2). The absence of Pro in TM5 of $S1P_1R$ leads to a regular a-helical conformation (∼3.6 residues per turn). Thus, the alignment of the $S1P_1R$ sequence to the other receptors requires two-residue gap relative to $A_{2A}R$ and one-residue gap relative to all other structures, which overlays $Y^{5.37}$ (*i-13* relative to $P^{5.50}$) of $A_{2A}R$ with $F/Y^{5.38}$ of the $P^{5.50}$-containing structures (*i-12* relative to $P^{5.50}$) and $F/Y/W^{5.39}$ of the $P^{5.50}$-lacking structures (Fig. 2.2).

2.4.6 Transmembrane Helix 6

TM6 presents the most pronounced kink in the TM bundle. This severe distortion is energetically stabilized through two structural and functional elements. First, $P^{6.50}$ of the highly conserved $CWxP^{6.50}(Y/F)$ motif introduces a flexible point in TM6 facilitating this extreme conformation. Second, a structural water molecule located in a small cavity between TMs 6 and 7 help to maintain the Pro induced distortion. This water acts as a hydrogen-bond acceptor in the interaction with the backbone N-H amide at position 6.51, and as a hydrogen bond donor in the interactions with the backbone carbonyl at position 6.47 and 7.38. Thus, in addition to stabilizing the kink of TM6, this water molecule links TMs 6 and 7.

2.4.7 Transmembrane Helix 7

TM7 start at different position among receptors. TM7 in CXCR4 is two helical turns longer than in other GPCRs. In this case, the longer TM7 allows $C^{7.25}$ to be placed at the tip of the helix in a favorable position to form a disulphide bond with Cys28 in the N-terminal region. TM7 is kinked at $P^{7.50}$ of the highly conserved NPxxY motif. This region of TM7, involved in key conformational changes associated with GPCR activation (Rosenbaum et al. 2009), is highly irregular. A network of water molecules stabilizes the helical deformation of TM7 and provides hydrogen-bonding partners to polar side chains. For instance, the unusual $P^{7.50}$ deformation removes the intrahelical hydrogen bond between the carbonyl group and the N-H amide at positions 7.45 and 7.49, respectively. A conserved water molecule is located between the backbone carbonyl at position 7.45 and the backbone N-H amide at position 7.49.

2.5 The Extracellular Surface in Class A G Protein-Coupled Receptors

The extracellular surface of GPCRs is defined by the conformation of the N-terminus region and ECLs1-3. Notably, the N-terminus and ECL2 in particular are highly variable in sequence, length, and structure (Peeters et al. 2011) (Fig. 2.4). In rhodopsin, the N-terminus (formed by two β-strands) and ECL2 (two β-strands) block the access of the extracellular ligand to the core of the receptor (Palczewski et al. 2000). Similarly, in $S1P_1R$, the N-terminus (contains a short α-helix) covers half the binding pocket and ECL2 (formed by a family-specific disulphide bridge within ECL 2, but lacking the conserved disulphide bridge between TM3 and ECL 2) covers the other half (Hanson et al. 2012). In these cases, retinal (Hildebrand et al. 2009; Park et al. 2008) and sphingosine-1-phosphate (Hanson et al. 2012) may gain access to the binding pocket from the lipid bilayer (Martin-Couce et al. 2012). In contrast, ECL2 in biogenic amine receptors, adenosine and peptide receptors adopt different spatial conformations that maintain the binding site rather accessible from the extracellular environment (Fig. 2.4). ECL2 of peptide receptors are formed by two β-strands, whereas a helical segment forms ECL2 of adrenergic receptors. This α-helix between TM4 and the disulphide bridge is not conserved in the other members of the biogenic amine receptor family. Thus, each receptor subfamily has probably developed, during evolution, a specific N-terminus/ECL2 to adjust the structural characteristics of its cognate ligands, and to

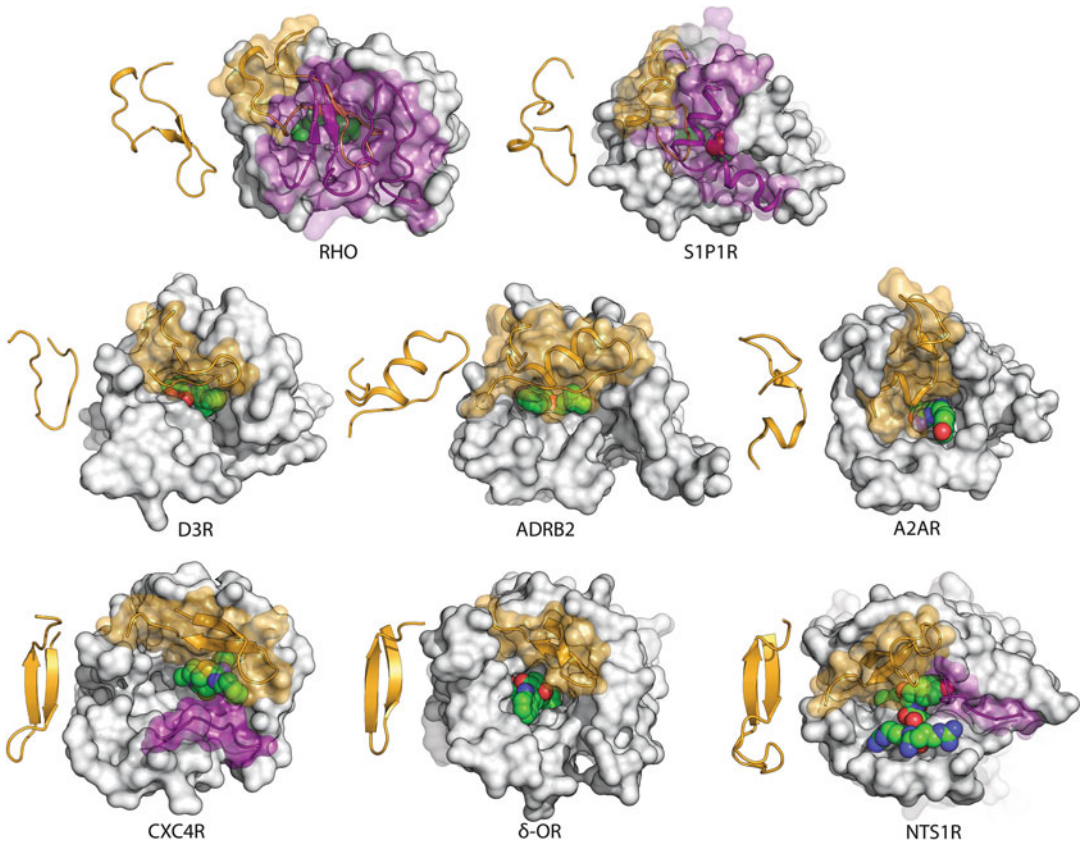

Fig. 2.4 Molecular surface of the extracellular domain in known crystal structures of GPCRs. The N-terminus domain is shown in *red*, ECL2 is shown in *yellow*, and the ligand in the binding site is shown as *spheres*

modulate the ligand binding/unbinding events (Hurst et al. 2010; Dror et al. 2011; Gonzalez et al. 2011).

2.6 Ligand Binding to G Protein-Coupled Receptors

Analysis of the known crystal structures of GPCRs shows that ligand binding mostly occurs in a main cavity located between the extracellular segments of TMs 3, 5, 6, and 7 or in a minor binding cavity located between the extracellular segments of TMs 1, 2, 3, and 7 (Rosenkilde et al. 2010) (Fig. 2.5a). Despite these common pockets, different ligands penetrate to different depths within the TM bundle (Venkatakrishnan et al. 2013) (Fig. 2.5b–f). A major issue in these common binding modes is the specificity of ligands among subfamilies of receptors.

2.7 Intracellular Structural Changes Associated with Activation of G Protein-Coupled Receptors

The publication of the crystal structure of the ligand-free opsin (Park et al. 2008), which contains several distinctive features of the active state as it has been confirmed in the recent structure of the β_2-adrenergic receptor bound to Gs (Rasmussen et al. 2011b), showed that during the process of receptor activation the intracellular part of TM6 tilts outwards, TM5 nears TM6, and $R^{3.50}$ within the (D/E)RY motif in TM3 adopts an extended conformation pointing towards the protein core, to interact with the highly conserved $Y^{5.58}$ in TM5 and $Y^{7.53}$ of the (N/D)PxxY motif in TM7 (Fig. 2.6). As shown in the original publication of the opsin structure, these conformational

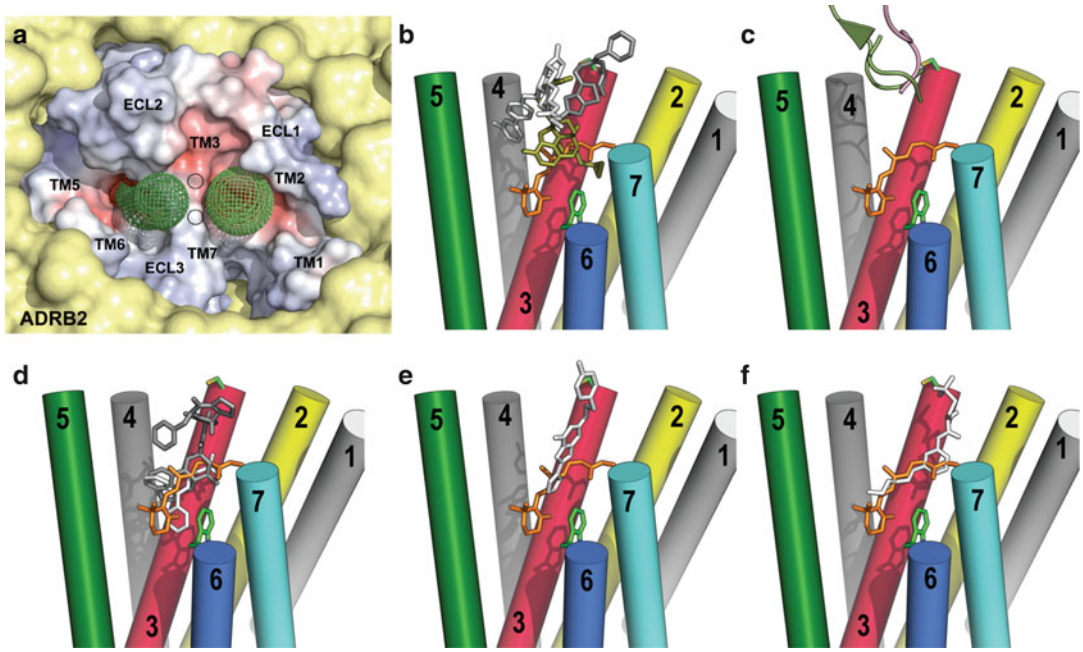

Fig. 2.5 Ligand binding to GPCRs. (**a**) Binding cavities in β_2AR. (**b**) The binding of vorapaxar (*white*) to PAR1 (Zhang et al. 2012), IT1t (*gray*) to CXCR4 (Wu et al. 2010), and morphinan (*olive*) to μ-OR (Manglik et al. 2012). (**c**) The binding of the CVX15 cyclic peptide (*olive*) to CXCR4 (Wu et al. 2010) and aminoacids 8–13 of neurotensin (*pink*) to NTSR1 (White et al. 2012). (**d**) The binding of doxepin (*white*) to H_1R (Shimamura et al. 2011) and ergotamine (*gray*) to $5HT_{1b}$R (Wang et al. 2013a). (**e**) The binding of ZM241385 (*white*) to A_{2A}R (Jaakola et al. 2008). (**f**) The binding of ML056 to $S1P_1$R (Hanson et al. 2012). The structures of retinal (*orange sticks*) and $C^{3.25}$ and $W^{6.48}$ (*green sticks*) are shown in panels B-F for comparison purposes

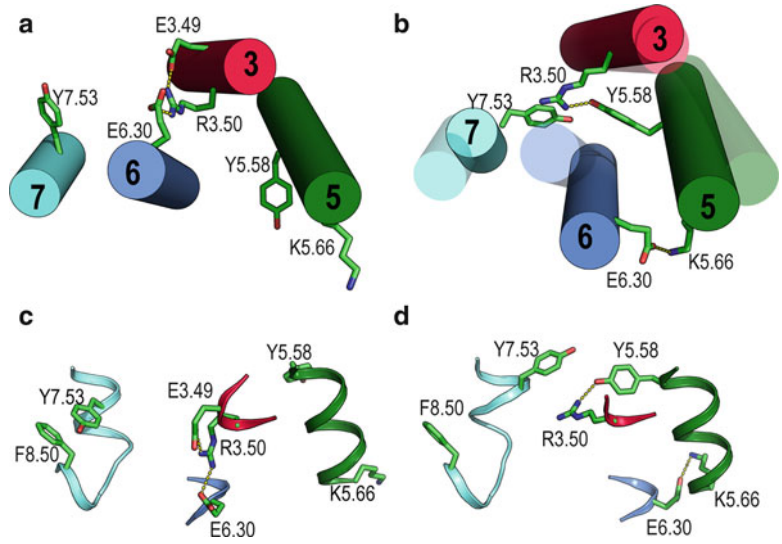

Fig. 2.6 Intracellular structural changes associated with receptor activation. Comparison of (**a, c**) the crystal structure of inactive rhodopsin (1GZM) with (**b, d**) the crystal structure of the ligand-free opsin (3CAP), which contains several distinctive features of the active state, in views parallel (**c, d**) and perpendicular (**a, b**) to the membrane. Panel *B* shows the positions of TMs 3, 5–7 in rhodopsin (transparent cylinders) and opsin (opaque cylinders) for comparison purposes

changes disrupt the ionic interaction between $R^{3.50}$ with negatively charged side chains at positions 3.49 in TM3 and 6.30 in TM6 (Fig. 2.6a, c) and facilitates the interaction between $K^{5.66}$ in TM 5 and $E^{6.30}$ in TM 6 (Fig. 2.6b, d). It has been suggested that conserved hydrophobic amino acids in the environment of these key polar residues form hydrophobic cages, which also restrain GPCRs in inactive conformations (Caltabiano et al. 2013).

2.8 Mechanism of Ligand-Induced G Protein-Coupled Receptor Activation

The crystal structure of a nanobody-stabilized active state of the β_2-adrenergic receptor bound to the BI-167107 agonist (Rasmussen et al. 2011a) shows hydrogen bonding interactions with $S^{5.42}$ and $S^{5.46}$ (Fig. 2.7a). These interactions stabilize a receptor conformation that includes a 2.1 Å inward movement of TM5 at position 5.46 and 1.4 Å inward movement of the conserved $P^{5.50}$ relative to the inactive, carazolol-bound structure (Rosenbaum et al. 2007). This key distortion is stabilized in the known crystal structures by a bulky hydrophobic side chain at position 3.40 (Fig. 2.7a), highly conserved in the whole Class A GPCR family (I:40 %, V:25 %, L:11 %). Mutation of $I^{3.40}$ to either Ala or Gly, i.e. removing the bulky side chain at this position, abolishes the constitutive activity of the histamine H_1 receptor, the effect of constitutive-activity increasing mutations, as well as the histamine-induced receptor activation (Sansuk et al. 2011). Thus, the inward movement of $P^{5.50}$ upon agonist binding repositions $I^{3.40}$ and $F^{6.44}$, which contributes to a rotation and outward movement of TM6 for receptor activation (Rasmussen et al. 2011a).

The structures of metarhodopsin II (Choe et al. 2011), the constitutively active rhodopsin (Standfuss et al. 2011) and the A_{2A} adenosine receptor in complex with the agonist UK-432097 (Xu et al. 2011) have shown that $W^{6.48}$ moves toward TM5 relative to the inactive structures (Fig. 2.7b), facilitating the rotation and tilt of the intracellular part of TM6.

The role of the extracellular domain in receptor function still remains unclear. However, NMR studies on the β_2-adrenergic receptor have shown ligand-specific conformational changes on the extracellular domain (Bokoch et al. 2010). Similarly, it has recently been reported that a

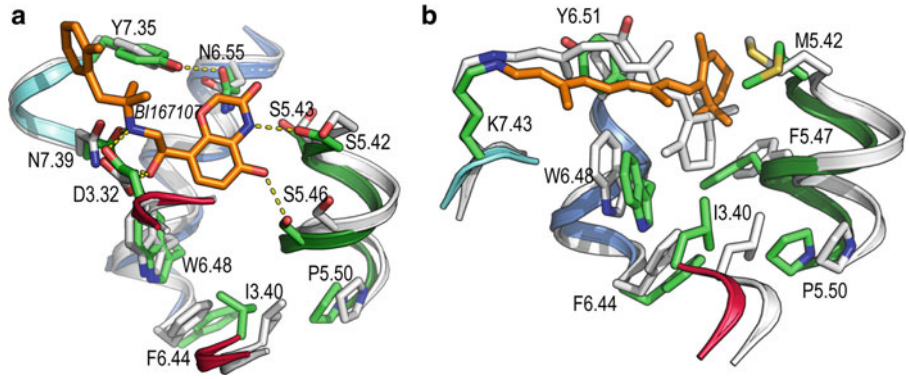

Fig. 2.7 Mechanisms of ligand-induced receptor activation. (**a**) Detailed view of the β_2-adrenergic receptor bound to the full agonist BI-167107 (in *orange*). The hydrogen bond interaction between full agonists and $S^{5.46}$ stabilizes a receptor conformation that includes an inward movement of TM5 relative to the inactive (shown in *white* for comparison purposes), carazolol-boundstructure. (**b**) The conformational change of inactive 11-*cis* retinal (in *white*) to the active 11-*trans* retinal (in *orange*) stabilizes a receptor conformation that includes an inward movement of TM5 together with a movement of $W^{6.48}$ toward TM5 relative to the inactive structures (shown in *white* for comparison purposes)

small cavity (vestibule) present at the entrance of the ligand-binding cavity controls the extent of receptor movement to govern a hierarchical order of G-protein coupling (Bock et al. 2012). Finally, the N-terminal domain of melanocortin receptors plays a significant role in their constitutive, ligand-independent, activity (Ersoy et al. 2012).

2.9 G Protein-Coupled Receptor Oligomerization

GPCRs have been classically described as monomeric TM receptors that form a ternary complex: a ligand, the GPCR, and its associated G protein. This is compatible with observations that monomeric rhodopsin and β_2-adrenergic receptor are capable of activating G proteins (Ernst et al. 2007; Whorton et al. 2007). Nevertheless, it is now well accepted that many GPCRs have been observed to oligomerize in cells (Pin et al. 2007; Ferre et al. 2009). It has been shown that receptor activation is modulated by allosteric communication between protomers of dopamine class A GPCR dimers (Han et al. 2009). The minimal signaling unit, two receptors and a single G protein, is maximally activated by agonist binding to a single protomer. Inverse agonist binding to the second protomer enhances signaling, whereas agonist binding to the second protomer blunts signaling. Moreover, binding of agonists or the G protein to β_2- regulates receptor oligomerization (Fung et al. 2009). Cysteine cross-linking experiments have suggested that receptor oligomerization involves hydrophobic interactions via the surfaces of TMs1, 4, and/or 5 (Klco et al. 2003; Guo et al. 2005, 2008). Nevertheless, electrostatic interactions of the intracellular domains are key in the formation of receptor heteromers (Navarro et al. 2010).

The recent release of the high-resolution crystal structures of μOR (Manglik et al. 2012) and β_1-AR (Huang et al. 2013) in the form of homo-oligomers (Fig. 2.8) facilitates the task of modeling GPCR dimers and higher order oligomers. The structure of μOR shows receptor molecules associated into pairs through two different interfaces (Fig. 2.8a). The first interface is via TMs1 and 2 and Hx8, and the second interface comprises TMs 5 and 6. The structure of β_1-AR contains a similar TMs1 and 2 and Hx8 interface but the other interface engages residues from TMs4 and 5 (Fig. 2.8b).

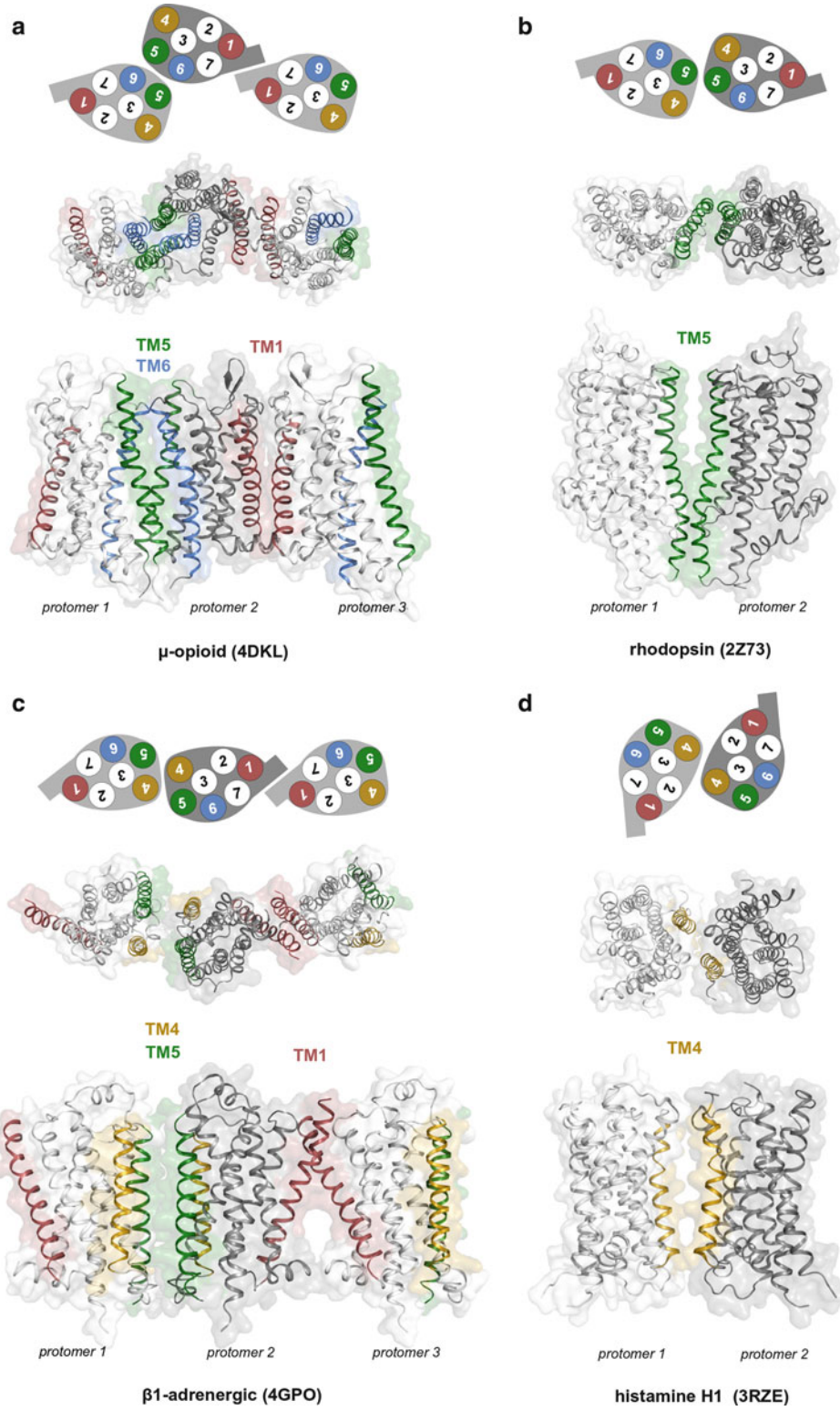

Fig. 2.8 GPCR oligomerization. The recent high-resolution crystal structures of (**a**) μOR (Manglik et al. 2012) and (**b**) β_1-AR (Huang et al. 2013) in the form of homo-oligomers, and sRho (Murakami and Kouyama 2008) and H_1R (Shimamura et al. 2011) in the form of homo-dimers

Additional crystal structures with GPCR dimers have been published. Interestingly, a TM1 interface, similar to the one observed for μOR and β_1-AR, is present in the structures of the κOR (Wu et al. 2012), opsin (Scheerer et al. 2008), and metarhodopsin II (Choe et al. 2011). Moreover, the TM4/5 interface of β_1-AR resembles the interface previously obtained for rhodopsin using atomic force microscopy (Fotiadis et al. 2003). The crystal structure of the histamine H_1 receptor (Shimamura et al. 2011) contains a TM4 interface (Fig. 2.8d), which is different from the TM4/5 interface of β_1-AR due to the absence of TM5 contacts. Similarly, the structures of CXCR4 (Wu et al. 2010) and squid rhodopsin (Murakami and Kouyama 2008) contain a TM5 interface (Fig. 2.8c), which are different from the TM4/5 interface of β_1-AR or the TM5/6 interface of μOR.

2.10 The Binding of G Protein-Coupled Receptors to the G Protein

The formation of the complex between the active conformation of the receptor and the heterotrimeric G protein triggers GDP release from the Gα-subunit, GTP binding to the Gα-subunit and dissociation of the Gβγ-subunits (Chung et al. 2011), which finally leads to a cascade of signals depending on the G-protein type. Noteworthy, more than 800 known GPCRs can bind 17 different Gα subunits, which have been grouped into four different classes ($G\alpha_s$, $G\alpha_i$, $G\alpha_q$ and $G\alpha_{12}$) (Simon et al. 1991). To date, the crystal structures of the ligand-free opsin (Scheerer et al. 2008), metarhodopsin II (Choe et al. 2011) and the constitutively active rhodopsin mutant $E^{3.28}Q$ (Standfuss et al. 2011) in complex with a peptide derived from the carboxy terminus of the α-subunit of the G protein transducin, together with the structure of the β_2-adrenergic receptor bound to Gs (Rasmussen et al. 2011b) have been released. These structures have shown that the C-terminal α5 helix of Gα binds to the intracellular cavity that is opened by the movement of the cytoplasmic end of TM6 away from TM3 and towards TM5 (see above). The C-terminal α5 helix of the α-subunit interacts with the extended conformation of $R^{3.50}$, the short loop connecting TM7 and Hx8, and the inner side of the cytoplasmic TMs 5 and 6 (Fig. 2.9).

2.11 The Binding of the C-Tail of G Protein-Coupled Receptors to Arrestin

Phosphorylation of several residues of the C-tail of GPCRs, by Ser/Thr kinases called G protein-coupled receptor kinases (GRKs), promotes the interactions between the receptor and arrestin, leading to receptor desensitization (Lefkowitz and Shenoy 2005). GPCRs can bind four different arrestin proteins: arrestin-1 and arrestin-4 (known as visual arrestins) bind to the phosphorylated form of active rhodopsin, whereas arrestin-2 and arrestin-3 interact and regulate the activity of non-visual GPCRs (Gurevich and Gurevich 2006).

Arrestin comprises two domains (N- and C- domains) of antiparallel β-sheets connected through a hinge region (Granzin et al. 1998) (Fig. 2.10). The binding region for phosphorylated ligand-activated receptor is located at the N-terminal domain, which is occupied by the long C-terminal tail in the basal state (blue peptide in Fig. 2.10a). The crystal structure of arrestin-2 in complex with a phosphorylated 29-aminoacid carboxy-terminal peptide derived from the human V2 vasopressin receptor (V2Rpp) (Shukla et al. 2013) has recently released. This structure shows that the phosphorylated C-tail region of GPCRs (yellow peptide in Fig. 2.10a) displaces the C-tail of arrestin. Moreover, an active conformation of arrestin-1, mimicked by C-tail truncation, has also been published (Kim et al. 2013). Both structures show significant conformational changes relative to inactive, basal, arrestin. These include rotation of the N- and C-terminal

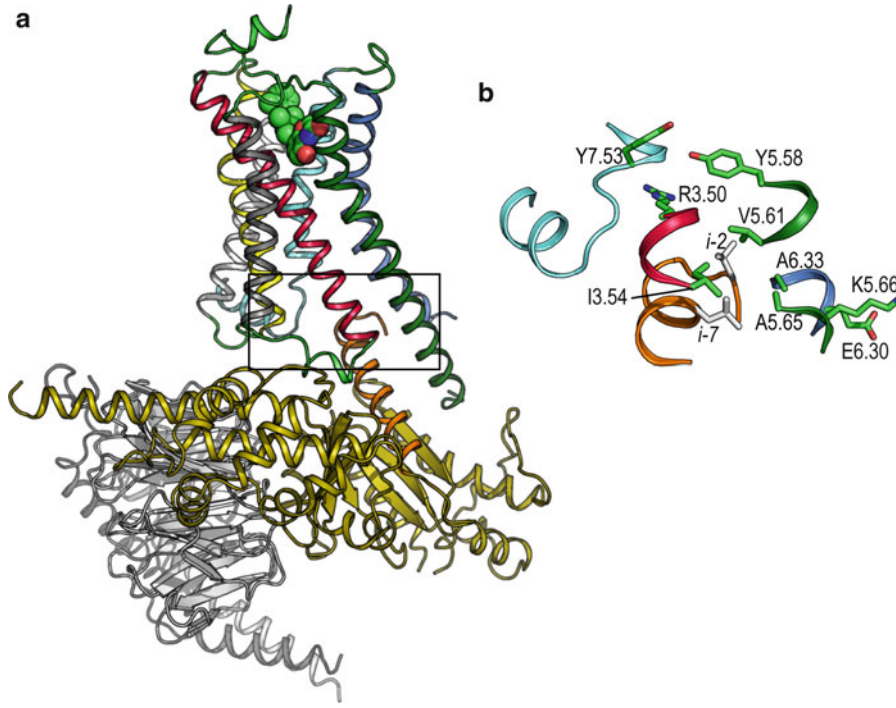

Fig. 2.9 G-protein binding. (**a**) Crystal structure of the β_2-adrenergic receptor in complex with the Gs heterotrimer (α-subunit in *olive*, β-subunit in *white*, and γ-subunit in *gray*). The C-terminal α5 helix of the α-subunit is shown in *orange*. The *rectangle* shows the part of the complex depicted in *panel B*. (**b**) Detailed view of the interaction between the C-terminal α5 helix of the α-subunit (in *orange*) with the short loop connecting TM7 and Hx8 (*light blue*), TM3 (*red*), and the inner side of the cytoplasmic TMs 5 (*green*) and 6 (*blue*)

domains relative to each other, and major reorientations of the lariat, middle, and finger loops (Fig. 2.10b).

2.12 Conclusions

GPCRs are disordered allosteric proteins that exhibit modulator behavior with a number of guests in both the extracellular (ligand) and intracellular (G protein, arrestin) spaces (Kenakin and Miller 2010). This considers GPCRs as monomeric TM receptors. Nevertheless, it is now well accepted that many GPCRs form homo- and hetero-oligomers (Khelashvili et al. 2010). Since 2007, innovative crystallographic techniques (Venkatakrishnan et al. 2013) have resulted in an exponential growth in the number of solved structures that include several members of the GPCR family (bound to either agonists, antagonists, or inverse agonists), in the form of monomers or homo-oligomers, in complex with the G protein, or the C-tail bound to arrestin. Thus, the used of these structures as templates allows molecular modelers to simulate the process of signal transduction through the cell membrane. These tailor-made models can study ligand binding, receptor specificity, receptor activation, G protein coupling, allosteric communication among protomers, among others. However, we want to emphasize that homology modeling of GPCRs is far from being a routine technique. Clearly, the inclusion of experimental results can improve the reliability of the models, and their predictive character.

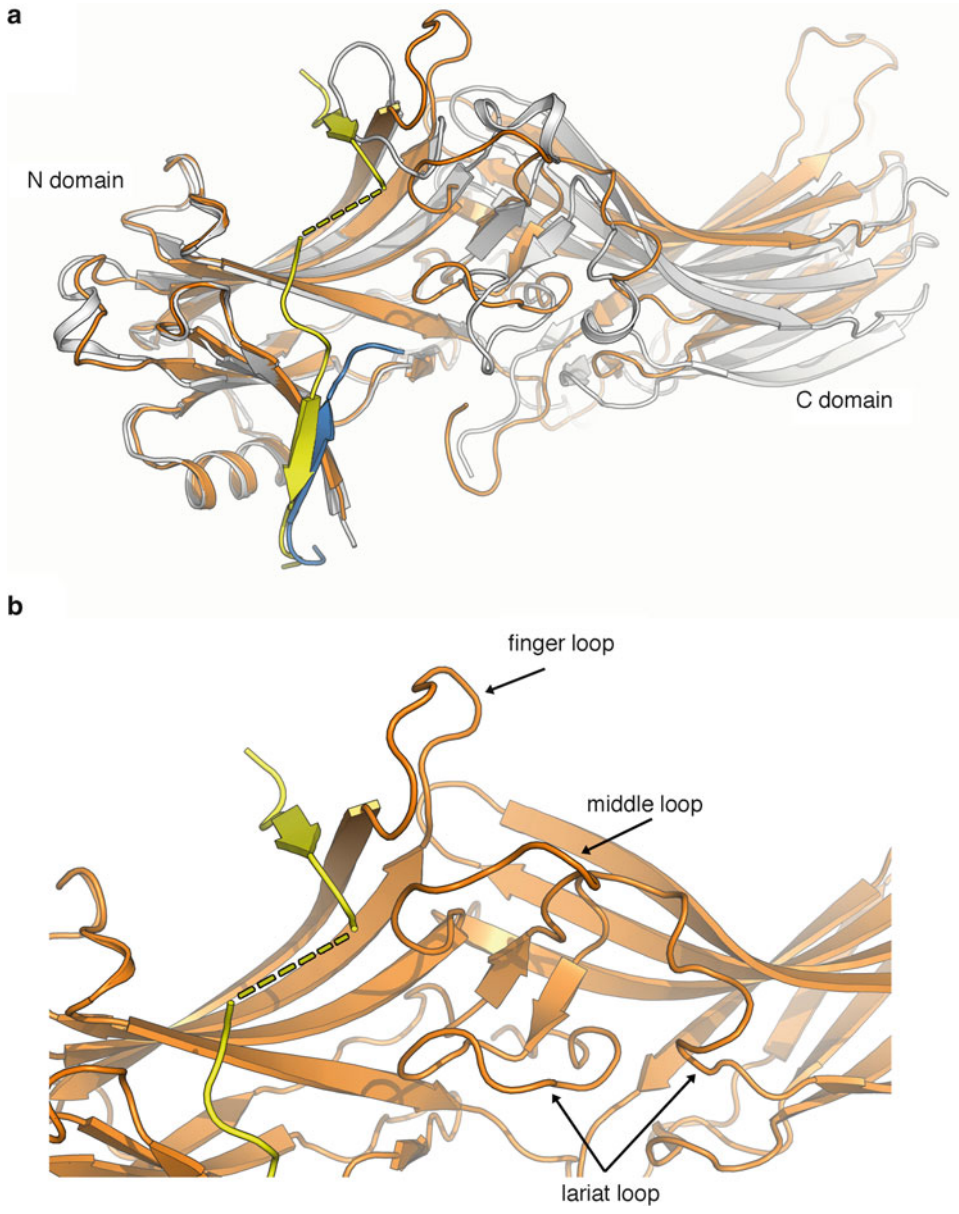

Fig. 2.10 The binding of the C-tail of GPCRs to arrestin. (**a**) The active conformation of arrestin-2 (PDB id 4JQI, shown in *orange*) is superimposed to inactive arrestin-2 (1G4M, in *gray*). The phosphorylated C-tail region of GPCRs (*yellow peptide*) displaces the C-tail of inactive arrestin (*blue peptide*). (**b**) Detailed view of the finger, middle and lariat loops, in the presumably active conformation of arrestin-2, which interact with the phosphorylated C-tail of GPCRs

References

Arinaminpathy Y, Khurana E, Engelman DM, Gerstein MB (2009) Computational analysis of membrane proteins: the largest class of drug targets. Drug Discov Today 14(23–24):1130–1135

Ballesteros JA, Weinstein H (1995) Integrated methods for the construction of three dimensional models and computational probing of structure-function relations in G-protein coupled receptors. Methods Neurosci 25:366–428

Blattermann S, Peters L, Ottersbach PA, Bock A, Konya V, Weaver CD, Gonzalez A, Schroder R, Tyagi R,

Luschnig P, Gab J, Hennen S, Ulven T, Pardo L, Mohr K, Gutschow M, Heinemann A, Kostenis E (2012) A biased ligand for OXE-R uncouples G alpha and G beta gamma signaling within a heterotrimer. Nat Chem Biol 8(7):631–638

Bock A, Merten N, Schrage R, Dallanoce C, Batz J, Klockner J, Schmitz J, Matera C, Simon K, Kebig A, Peters L, Muller A, Schrobang-Ley J, Trankle C, Hoffmann C, De Amici M, Holzgrabe U, Kostenis E, Mohr K (2012) The allosteric vestibule of a seven transmembrane helical receptor controls G-protein coupling. Nat Commun 3:1044

Bokoch MP, Zou Y, Rasmussen SG, Liu CW, Nygaard R, Rosenbaum DM, Fung JJ, Choi HJ, Thian FS, Kobilka TS, Puglisi JD, Weis WI, Pardo L, Prosser RS, Mueller L, Kobilka BK (2010) Ligand-specific regulation of the extracellular surface of a G-protein-coupled receptor. Nature 463(7277):108–112

Caltabiano G, Gonzalez A, Cordomi A, Campillo M, Pardo L (2013) The role of hydrophobic amino acids in the structure and function of the rhodopsin family of G protein-coupled receptors. Methods Enzymol 520:99–115

Cherezov V, Rosenbaum DM, Hanson MA, Rasmussen SG, Thian FS, Kobilka TS, Choi HJ, Kuhn P, Weis WI, Kobilka BK, Stevens RC (2007) High-resolution crystal structure of an engineered human beta2-adrenergic G protein-coupled receptor. Science 318(5854):1258–1265

Chien EY, Liu W, Zhao Q, Katritch V, Han GW, Hanson MA, Shi L, Newman AH, Javitch JA, Cherezov V, Stevens RC (2010) Structure of the human dopamine D3 receptor in complex with a D2/D3 selective antagonist. Science 330(6007):1091–1095

Choe HW, Kim YJ, Park JH, Morizumi T, Pai EF, Krauss N, Hofmann KP, Scheerer P, Ernst OP (2011) Crystal structure of metarhodopsin II. Nature 471(7340):651–655

Choma C, Gratkowski H, Lear JD, DeGrado WF (2000) Asparagine-mediated self-association of a model transmembrane helix. Nat Struct Biol 7(2):161–166

Chung KY, Rasmussen SG, Liu T, Li S, DeVree BT, Chae PS, Calinski D, Kobilka BK, Woods VL Jr, Sunahara RK (2011) Conformational changes in the G protein Gs induced by the beta2 adrenergic receptor. Nature 477(7366):611–615

Day PW, Rasmussen SG, Parnot C, Fung JJ, Masood A, Kobilka TS, Yao XJ, Choi HJ, Weis WI, Rohrer DK, Kobilka BK (2007) A monoclonal antibody for G protein-coupled receptor crystallography. Nat Methods 4(11):927–929

de la Fuente T, Martin-Fontecha M, Sallander J, Benhamu B, Campillo M, Medina RA, Pellissier LP, Claeysen S, Dumuis A, Pardo L, Lopez-Rodriguez ML (2010) Benzimidazole derivatives as new serotonin 5-HT(6) receptor antagonists. Molecular mechanisms of receptor inactivation. J Med Chem 53(3):1357–1369

Deupi X, Olivella M, Govaerts C, Ballesteros JA, Campillo M, Pardo L (2004) Ser and Thr residues modulate the conformation of pro-kinked transmembrane alpha-helices. Biophys J 86(1):105–115

Deupi X, Dolker N, Lopez-Rodriguez M, Campillo M, Ballesteros J, Pardo L (2007) Structural models of class a G protein-coupled receptors as a tool for drug design: insights on transmembrane bundle plasticity. Curr Top Med Chem 7(10):999–1006

Deupi X, Olivella M, Sanz A, Dolker N, Campillo M, Pardo L (2010) Influence of the g- conformation of Ser and Thr on the structure of transmembrane helices. J Struct Biol 169(1):116–123

Deville J, Rey J, Chabbert M (2009) An indel in transmembrane helix 2 helps to trace the molecular evolution of class A G-protein-coupled receptors. J Mol Evol 68(5):475–489

Dror RO, Pan AC, Arlow DH, Borhani DW, Maragakis P, Shan Y, Xu H, Shaw DE (2011) Pathway and mechanism of drug binding to G-protein-coupled receptors. Proc Natl Acad Sci U S A 108(32):13118–13123

Ernst OP, Gramse V, Kolbe M, Hofmann KP, Heck M (2007) Monomeric G protein-coupled receptor rhodopsin in solution activates its G protein transducin at the diffusion limit. Proc Natl Acad Sci U S A 104(26):10859–10864

Ersoy BA, Pardo L, Zhang S, Thompson DA, Millhauser G, Govaerts C, Vaisse C (2012) Mechanism of N-terminal modulation of activity at the melanocortin-4 receptor GPCR. Nat Chem Biol 8(8):725–730

Ferre S, Baler R, Bouvier M, Caron MG, Devi LA, Durroux T, Fuxe K, George SR, Javitch JA, Lohse MJ, Mackie K, Milligan G, Pfleger KD, Pin JP, Volkow ND, Waldhoer M, Woods AS, Franco R (2009) Building a new conceptual framework for receptor heteromers. Nat Chem Biol 5(3):131–134

Fotiadis D, Liang Y, Filipek S, Saperstein DA, Engel A, Palczewski K (2003) Atomic-force microscopy: rhodopsin dimers in native disc membranes. Nature 421(6919):127–128

Fredriksson R, Schioth HB (2005) The repertoire of G-protein-coupled receptors in fully sequenced genomes. Mol Pharmacol 67(5):1414–1425

Fung JJ, Deupi X, Pardo L, Yao XJ, Velez-Ruiz GA, Devree BT, Sunahara RK, Kobilka BK (2009) Ligand-regulated oligomerization of beta(2)-adrenoceptors in a model lipid bilayer. EMBO J 28(21):2384–2392

Gonzalez A, Perez-Acle T, Pardo L, Deupi X (2011) Molecular basis of ligand dissociation in beta-adrenergic receptors. PLoS One 6(9):e23815

Gonzalez A, Cordomí A, Caltabiano G, Campillo M, Pardo L (2012) Impact of helix irregularities on sequence alignment and homology modelling of G protein-coupled receptors. Chembiochem 13(10):1393–1399

Granier S, Manglik A, Kruse AC, Kobilka TS, Thian FS, Weis WI, Kobilka BK (2012) Structure of the delta-opioid receptor bound to naltrindole. Nature 485(7398):400–404

Granzin J, Wilden U, Choe HW, Labahn J, Krafft B, Buldt G (1998) X-ray crystal structure of arrestin from bovine rod outer segments. Nature 391(6670):918–921

Guo W, Shi L, Filizola M, Weinstein H, Javitch JA (2005) Crosstalk in G protein-coupled receptors:

changes at the transmembrane homodimer interface determine activation. Proc Natl Acad Sci U S A 102:17495–17500

Guo W, Urizar E, Kralikova M, Mobarec JC, Shi L, Filizola M, Javitch JA (2008) Dopamine D2 receptors form higher order oligomers at physiological expression levels. EMBO J 27(17):2293–2304

Gurevich VV, Gurevich EV (2006) The structural basis of arrestin-mediated regulation of G-protein-coupled receptors. Pharmacol Ther 110(3):465–502

Haga K, Kruse AC, Asada H, Yurugi-Kobayashi T, Shiroishi M, Zhang C, Weis WI, Okada T, Kobilka BK, Haga T, Kobayashi T (2012) Structure of the human M2 muscarinic acetylcholine receptor bound to an antagonist. Nature 482(7386):547–551

Han Y, Moreira IS, Urizar E, Weinstein H, Javitch JA (2009) Allosteric communication between protomers of dopamine class A GPCR dimers modulates activation. Nat Chem Biol 5(9):688–695

Hanson MA, Roth CB, Jo E, Griffith MT, Scott FL, Reinhart G, Desale H, Clemons B, Cahalan SM, Schuerer SC, Sanna MG, Han GW, Kuhn P, Rosen H, Stevens RC (2012) Crystal structure of a lipid G protein-coupled receptor. Science 335(6070):851–855

Hildebrand PW, Scheerer P, Park JH, Choe HW, Piechnick R, Ernst OP, Hofmann KP, Heck M (2009) A ligand channel through the G protein coupled receptor opsin. PLoS One 4(2):e4382

Hopf TA, Colwell LJ, Sheridan R, Rost B, Sander C, Marks DS (2012) Three-dimensional structures of membrane proteins from genomic sequencing. Cell 149(7):1607–1621

Huang J, Chen S, Zhang JJ, Huang XY (2013) Crystal structure of oligomeric beta1-adrenergic G protein-coupled receptors in ligand-free basal state. Nat Struct Mol Biol 20(4):419–425

Hurst DP, Grossfield A, Lynch DL, Feller S, Romo TD, Gawrisch K, Pitman MC, Reggio PH (2010) A lipid pathway for ligand binding is necessary for a cannabinoid G protein-coupled receptor. J Biol Chem 285(23):17954–17964

Imming P, Sinning C, Meyer A (2006) Drugs, their targets and the nature and number of drug targets. Nat Rev Drug Discov 5(10):821–834

Jaakola VP, Griffith MT, Hanson MA, Cherezov V, Chien EY, Lane JR, Ijzerman AP, Stevens RC (2008) The 2.6 angstrom crystal structure of a human A2A adenosine receptor bound to an antagonist. Science 322(5905):1211–1217

Katritch V, Cherezov V, Stevens RC (2012) Diversity and modularity of G protein-coupled receptor structures. Trends Pharmacol Sci 33(1):17–27

Katritch V, Cherezov V, Stevens RC (2013) Structure-function of the G protein-coupled receptor superfamily. Annu Rev Pharmacol Toxicol 53:531–556

Kenakin T, Miller LJ (2010) Seven transmembrane receptors as shapeshifting proteins: the impact of allosteric modulation and functional selectivity on new drug discovery. Pharmacol Rev 62(2):265–304

Khelashvili G, Dorff K, Shan J, Camacho-Artacho M, Skrabanek L, Vroling B, Bouvier M, Devi LA, George SR, Javitch JA, Lohse MJ, Milligan G, Neubig RR, Palczewski K, Parmentier M, Pin JP, Vriend G, Campagne F, Filizola M (2010) GPCR-OKB: the G protein coupled receptor oligomer knowledge base. Bioinformatics 26(14):1804–1805

Kim YJ, Hofmann KP, Ernst OP, Scheerer P, Choe HW, Sommer ME (2013) Crystal structure of pre-activated arrestin p44. Nature 497(7447):142–146

Klco JM, Lassere TB, Baranski TJ (2003) C5a Receptor oligomerization. I. Disulfide trapping reveals oligomers and potential contact surfaces in a G protein-coupled receptor. J Biol Chem 278(37):35345–35353

Klco JM, Nikiforovich GV, Baranski TJ (2006) Genetic analysis of the first and third extracellular loops of the C5a receptor reveals an essential WXFG motif in the first loop. J Biol Chem 281(17):12010–12019

Krissinel E, Henrick K (2004) Secondary-structure matching (SSM), a new tool for fast protein structure alignment in three dimensions. Acta Crystallogr D Biol Crystallogr 60(Pt 12 Pt 1):2256–2268

Kristiansen K (2004) Molecular mechanisms of ligand binding, signaling, and regulation within the superfamily of G-protein-coupled receptors: molecular modeling and mutagenesis approaches to receptor structure and function. Pharmacol Ther 103(1):21–80

Kruse AC, Hu J, Pan AC, Arlow DH, Rosenbaum DM, Rosemond E, Green HF, Liu T, Chae PS, Dror RO, Shaw DE, Weis WI, Wess J, Kobilka BK (2012) Structure and dynamics of the M3 muscarinic acetylcholine receptor. Nature 482(7386):552–556

Lefkowitz RJ, Shenoy SK (2005) Transduction of receptor signals by beta-arrestins. Science 308(5721):512–517

Li J, Edwards PC, Burghammer M, Villa C, Schertler GF (2004) Structure of bovine rhodopsin in a trigonal crystal form. J Mol Biol 343(5):1409–1438

Liu W, Chun E, Thompson AA, Chubukov P, Xu F, Katritch V, Han GW, Roth CB, Heitman LH, IJzerman AP, Cherezov V, Stevens RC (2012) Structural basis for allosteric regulation of GPCRs by sodium ions. Science 337(6091):232–236

Manglik A, Kruse AC, Kobilka TS, Thian FS, Mathiesen JM, Sunahara RK, Pardo L, Weis WI, Kobilka BK, Granier S (2012) Crystal structure of the micro-opioid receptor bound to a morphinan antagonist. Nature 485(7398):321–326

Martin-Couce L, Martin-Fontecha M, Palomares O, Mestre L, Cordomi A, Hernangomez M, Palma S, Pardo L, Guaza C, Lopez-Rodriguez ML, Ortega-Gutierrez S (2012) Chemical probes for the recognition of cannabinoid receptors in native systems. Angewandte Chemie 51(28):6896–6899

Mirzadegan T, Benko G, Filipek S, Palczewski K (2003) Sequence analyses of G-protein-coupled receptors: similarities to rhodopsin. Biochemistry 42(10):2759–2767

Mobarec JC, Sanchez R, Filizola M (2009) Modern homology modeling of G-protein coupled receptors: which structural template to use? J Med Chem 52(16):5207–5216

Murakami M, Kouyama T (2008) Crystal structure of squid rhodopsin. Nature 453(7193):363–367

Navarro G, Ferre S, Cordomi A, Moreno E, Mallol J, Casado V, Cortes A, Hoffmann H, Ortiz J, Canela EI, Lluis C, Pardo L, Franco R, Woods AS (2010) Interactions between intracellular domains as key determinants of the quaternary structure and function of receptor heteromers. J Biol Chem 285(35):27346–27359

Oldham WM, Hamm HE (2008) Heterotrimeric G protein activation by G-protein-coupled receptors. Nat Rev Mol Cell Biol 9(1):60–71

Olivella M, Gonzalez A, Pardo L, Deupi X (2013) Relation between sequence and structure in membrane proteins. Bioinformatics 29(13):1589–1592. doi:10.1093/bioinformatics/btt249

Palczewski K, Kumasaka T, Hori T, Behnke CA, Motoshima H, Fox BA, Trong IL, Teller DC, Okada T, Stenkamp RE, Yamamoto M, Miyano M (2000) Crystal structure of rhodopsin: a G protein-coupled receptor. Science 289(5480):739–745

Pardo L, Deupi X, Dolker N, Lopez-Rodriguez ML, Campillo M (2007) The role of internal water molecules in the structure and function of the rhodopsin family of G protein-coupled receptors. Chembiochem 8(1):19–24

Park JH, Scheerer P, Hofmann KP, Choe HW, Ernst OP (2008) Crystal structure of the ligand-free G-protein-coupled receptor opsin. Nature 454(7201):183–187

Peeters MC, van Westen GJ, Li Q, Ijzerman AP (2011) Importance of the extracellular loops in G protein-coupled receptors for ligand recognition and receptor activation. Trends Pharmacol Sci 32(1):35–42

Pieper U, Schlessinger A, Kloppmann E, Chang GA, Chou JJ, Dumont ME, Fox BG, Fromme P, Hendrickson WA, Malkowski MG, Rees DC, Stokes DL, Stowell MH, Wiener MC, Rost B, Stroud RM, Stevens RC, Sali A (2013) Coordinating the impact of structural genomics on the human alpha-helical transmembrane proteome. Nat Struct Mol Biol 20(2):135–138

Pin JP, Neubig R, Bouvier M, Devi L, Filizola M, Javitch JA, Lohse MJ, Milligan G, Palczewski K, Parmentier M, Spedding M (2007) International union of basic and clinical pharmacology. LXVII. Recommendations for the recognition and nomenclature of G protein-coupled receptor heteromultimers. Pharmacol Rev 59(1):5–13

Rasmussen SG, Choi HJ, Fung JJ, Pardon E, Casarosa P, Chae PS, Devree BT, Rosenbaum DM, Thian FS, Kobilka TS, Schnapp A, Konetzki I, Sunahara RK, Gellman SH, Pautsch A, Steyaert J, Weis WI, Kobilka BK (2011a) Structure of a nanobody-stabilized active state of the beta(2) adrenoceptor. Nature 469(7329):175–180

Rasmussen SG, DeVree BT, Zou Y, Kruse AC, Chung KY, Kobilka TS, Thian FS, Chae PS, Pardon E, Calinski D, Mathiesen JM, Shah ST, Lyons JA, Caffrey M, Gellman SH, Steyaert J, Skiniotis G, Weis WI, Sunahara RK, Kobilka BK (2011b) Crystal structure of the beta2 adrenergic receptor-Gs protein complex. Nature 477(7366):549–555

Riek RP, Rigoutsos I, Novotny J, Graham RM (2001) Non-alpha-helical elements modulate polytopic membrane protein architecture. J Mol Biol 306(2):349–362

Rosenbaum DM, Cherezov V, Hanson MA, Rasmussen SG, Thian FS, Kobilka TS, Choi HJ, Yao XJ, Weis WI, Stevens RC, Kobilka BK (2007) GPCR engineering yields high-resolution structural insights into beta2-adrenergic receptor function. Science 318(5854):1266–1273

Rosenbaum DM, Rasmussen SG, Kobilka BK (2009) The structure and function of G-protein-coupled receptors. Nature 459(7245):356–363

Rosenkilde MM, Benned-Jensen T, Frimurer TM, Schwartz TW (2010) The minor binding pocket: a major player in 7TM receptor activation. Trends Pharmacol Sci 31(12):567–574

Sansuk K, Deupi X, Torrecillas IR, Jongejan A, Nijmeijer S, Bakker RA, Pardo L, Leurs R (2011) A structural insight into the reorientation of transmembrane domains 3 and 5 during family a G protein-coupled receptor activation. Mol Pharmacol 79(2):262–269

Scheerer P, Park JH, Hildebrand PW, Kim YJ, Krauss N, Choe HW, Hofmann KP, Ernst OP (2008) Crystal structure of opsin in its G-protein-interacting conformation. Nature 455(7212):497–502

Senes A, Gerstein M, Engelman DM (2000) Statistical analysis of amino acid patterns in transmembrane helices: the GxxxG motif occurs frequently and in association with β-branched residues at neighboring positions. J Mol Biol 296:921–936

Serrano-Vega MJ, Magnani F, Shibata Y, Tate CG (2008) Conformational thermostabilization of the beta1-adrenergic receptor in a detergent-resistant form. Proc Natl Acad Sci U S A 105(3):877–882

Shimamura T, Shiroishi M, Weyand S, Tsujimoto H, Winter G, Katritch V, Abagyan R, Cherezov V, Liu W, Han GW, Kobayashi T, Stevens RC, Iwata S (2011) Structure of the human histamine H1 receptor complex with doxepin. Nature 475(7354):65–70

Shukla AK, Manglik A, Kruse AC, Xiao K, Reis RI, Tseng WC, Staus DP, Hilger D, Uysal S, Huang LY, Paduch M, Tripathi-Shukla P, Koide A, Koide S, Weis WI, Kossiakoff AA, Kobilka BK, Lefkowitz RJ (2013) Structure of active beta-arrestin-1 bound to a G-protein-coupled receptor phosphopeptide. Nature 497(7447):137–141

Simon MI, Strathmann MP, Gautam N (1991) Diversity of G proteins in signal transduction. Science 252(5007):802–808

Smit MJ, Vischer HF, Bakker RA, Jongejan A, Timmerman H, Pardo L, Leurs R (2007) Pharmacogenomic and structural analysis of constitutive G protein-coupled receptor activity. Annu Rev Pharmacol Toxicol 47:53–87

Standfuss J, Edwards PC, D'Antona A, Fransen M, Xie G, Oprian DD, Schertler GF (2011) The structural basis of agonist-induced activation in constitutively active rhodopsin. Nature 471(7340):656–660

Thompson AA, Liu W, Chun E, Katritch V, Wu H, Vardy E, Huang XP, Trapella C, Guerrini R, Calo G, Roth

BL, Cherezov V, Stevens RC (2012) Structure of the nociceptin/orphanin FQ receptor in complex with a peptide mimetic. Nature 485(7398):395–399

Venkatakrishnan AJ, Deupi X, Lebon G, Tate CG, Schertler GF, Babu MM (2013) Molecular signatures of G-protein-coupled receptors. Nature 494(7436):185–194

Von Heijne G (1991) Proline kinks in transmembrane alpha-helices. J Mol Biol 218(3):499–503

Wacker D, Wang C, Katritch V, Han GW, Huang XP, Vardy E, McCorvy JD, Jiang Y, Chu M, Siu FY, Liu W, Xu HE, Cherezov V, Roth BL, Stevens RC (2013) Structural features for functional selectivity at serotonin receptors. Science 340(6132):615–619

Wang C, Jiang Y, Ma J, Wu H, Wacker D, Katritch V, Han GW, Liu W, Huang XP, Vardy E, McCorvy JD, Gao X, Zhou EX, Melcher K, Zhang C, Bai F, Yang H, Yang L, Jiang H, Roth BL, Cherezov V, Stevens RC, Xu HE (2013a) Structural basis for molecular recognition at serotonin receptors. Science 340(6132):610–614

Wang C, Wu H, Katritch V, Han GW, Huang XP, Liu W, Siu FY, Roth BL, Cherezov V, Stevens RC (2013b) Structure of the human smoothened receptor bound to an antitumour agent. Nature 497(7449):338–343

Warne T, Serrano-Vega MJ, Baker JG, Moukhametzianov R, Edwards PC, Henderson R, Leslie AG, Tate CG, Schertler GF (2008) Structure of a beta(1)-adrenergic G-protein-coupled receptor. Nature 454:486–491

Warne T, Moukhametzianov R, Baker JG, Nehme R, Edwards PC, Leslie AG, Schertler GF, Tate CG (2011) The structural basis for agonist and partial agonist action on a beta(1)-adrenergic receptor. Nature 469(7329):241–244

White JF, Noinaj N, Shibata Y, Love J, Kloss B, Xu F, Gvozdenovic-Jeremic J, Shah P, Shiloach J, Tate CG, Grisshammer R (2012) Structure of the agonist-bound neurotensin receptor. Nature 490(7421):508–513

Whorton MR, Bokoch MP, Rasmussen SG, Huang B, Zare RN, Kobilka B, Sunahara RK (2007) A monomeric G protein-coupled receptor isolated in a high-density lipoprotein particle efficiently activates its G protein. Proc Natl Acad Sci U S A 104(18):7682–7687

Wu B, Chien EY, Mol CD, Fenalti G, Liu W, Katritch V, Abagyan R, Brooun A, Wells P, Bi FC, Hamel DJ, Kuhn P, Handel TM, Cherezov V, Stevens RC (2010) Structures of the CXCR4 chemokine GPCR with small-molecule and cyclic peptide antagonists. Science 330(6007):1066–1071

Wu H, Wacker D, Mileni M, Katritch V, Han GW, Vardy E, Liu W, Thompson AA, Huang XP, Carroll FI, Mascarella SW, Westkaemper RB, Mosier PD, Roth BL, Cherezov V, Stevens RC (2012) Structure of the human kappa-opioid receptor in complex with JDTic. Nature 485(7398):327–332

Xu F, Wu H, Katritch V, Han GW, Jacobson KA, Gao ZG, Cherezov V, Stevens RC (2011) Structure of an agonist-bound human A2A adenosine receptor. Science 332(6027):322–327

Zhang C, Srinivasan Y, Arlow DH, Fung JJ, Palmer D, Zheng Y, Green HF, Pandey A, Dror RO, Shaw DE, Weis WI, Coughlin SR, Kobilka BK (2012) High-resolution crystal structure of human protease-activated receptor 1. Nature 492(7429):387–392